ETSI GR mWT 030 V0.0.1 (2023-05)

Propagation measurement and modelling for PtP radio links in the E, W and D bands

Disclaimer

The present document has been produced and approved by the millimetre Wave Transmission (mWT) ETSI Industry Specification Group (ISG) and represents the views of those members who participated in this ISG.
It does not necessarily represent the views of the entire ETSI membership.

Reference
DGR/mWT-012

Keywords
Antenna, millimetre wave, transmission,
backhaul, mWT

ETSI

650 Route des Lucioles
F-06921 Sophia Antipolis Cedex - FRANCE

Tel.: +33 4 92 94 42 00 Fax: +33 4 93 65 47 16

Siret N° 348 623 562 00017 - NAF 742 C
Association à but non lucratif enregistrée à la
Sous-préfecture de Grasse (06) N° 7803/88

Important notice

The present document can be downloaded from:
http://www.etsi.org/standards-search

The present document may be made available in electronic versions and/or in print. The content of any electronic and/or print versions of the present document shall not be modified without the prior written authorization of ETSI. In case of any existing or perceived difference in contents between such versions and/or in print, the only prevailing document is the print of the Portable Document Format (PDF) version kept on a specific network drive within ETSI Secretariat.

Users of the present document should be aware that the document may be subject to revision or change of status.
Information on the current status of this and other ETSI documents is available at
https://portal.etsi.org/TB/ETSIDeliverableStatus.aspx

If you find errors in the present document, please send your comment to one of the following services:
https://portal.etsi.org/People/CommiteeSupportStaff.aspx

Contents

Intellectual Property Rights

IPRs essential or potentially essential to the present document may have been declared to ETSI. The information pertaining to these essential IPRs, if any, is publicly available for **ETSI members and non-members**, and can be found in ETSI SR 000 314: *"Intellectual Property Rights (IPRs); Essential, or potentially Essential, IPRs notified to ETSI in respect of ETSI standards"*, which is available from the ETSI Secretariat. Latest updates are available on the ETSI Web server (https://ipr.etsi.org).

Pursuant to the ETSI IPR Policy, no investigation, including IPR searches, has been carried out by ETSI. No guarantee can be given as to the existence of other IPRs not referenced in ETSI SR 000 314 (or the updates on the ETSI Web server) which are, or may be, or may become, essential to the present document.

Foreword

This Group Report (GR) has been produced by ETSI Industry Specification Group (ISG) millimetre Wave Transmission (mWT).

Modal verbs terminology

In the present document "**should**", "**should not**", "**may**", "**need not**", "**will**", "**will not**", "**can**" and "**cannot**" are to be interpreted as described in clause 3.2 of the ETSI Drafting Rules (Verbal forms for the expression of provisions).

"**must**" and "**must not**" are **NOT** allowed in ETSI deliverables except when used in direct citation.

Executive summary

This report

Introduction

This report deals with electro-magnetic (EM) wave propagation at millimetre-wave (mmW) for terrestrial PtP links, with particular consideration of frequencies about and over 100 GHz, in the E (71-86 GHz), W (92-115 GHz) and D (130-175 GHz) bands. In this high frequency range propagation is subject to several atmospheric effects induced by:

- Gases (mainly oxygen and water vapour)
- Suspended water droplets (fog)
- Hydrometeors (rain, snow, hail)

Among them, rain plays the most relevant role since at frequencies higher than 10 GHz rain drops absorb and scatter electromagnetic energy, thus inducing significant path losses; this effect becomes more and more relevant as long as the wavelength begins to be comparable to the rain drop size (about 1 mm), in particular in the mmW part of the EM spectrum.

That's why it is of paramount importance to investigate atmospheric effects impairing millimeter-waves, specifically rain attenuation, which is greatly dependent on the operational frequency, on the rain rate and on the rain drop dimensions, described by the so called Drop Size Distribution (DSD).

Actually, there are two ITU-R Recommendations dealing with rain attenuation effects:

- ITU-R Recommendation P.838-3, which provides specific attenuation as a function of the rain rate and operational frequency
- ITU-R Recommendation P.530-18, which presents a rain attenuation model for terrestrial links

Both theoretical analysis and field measurements highlighted the importance of considering the microphysics of rain when predicting specific attenuation due to rain; this is currently not taken into account in ITU-R P.838-3.

Moreover when considering short radio links (in the order of a few hundred meters and up to 1 km), which would be typical when considering systems at D band, a proper evaluation of the spatial variation of rain rate along the link length should be performed; the effective path length over which the rain rate can be considered uniform is given by the link length multiplied by the so called path reduction factor and is highly dependent on the rain rate; in case of high rain rate, typical of convective events, the effective path length can be expected to be small, whilst for low rain rate, typical of stratiform events, the effective path length would tend to be large.

Both theoretical analysis and field measurements highlighted that in case of short radio links (less than 1 km) the path reduction factor should be less than or equal to 1, according to the rain rate; this is currently not true in the ITU-R P.530-18. It is also worth to be noted that the application of model in the ITU-R P.530-18 is recommended for operational frequencies up to 100 GHz.

1 Scope

The present document provides information about electromagnetic propagation at millimetre wave, considering the available models, both derived from physical analysis and from real data fitting and comparing them with measurements.

2 References

2.1 Normative references

Normative references are not applicable in the present document.

2.2 Informative references

References are either specific (identified by date of publication and/or edition number or version number) or non-specific. For specific references, only the cited version applies. For non-specific references, the latest version of the referenced document (including any amendments) applies.

NOTE: While any hyperlinks included in this clause were valid at the time of publication, ETSI cannot guarantee their long term validity.

The following referenced documents are not necessary for the application of the present document but they assist the user with regard to a particular subject area.

[i.1] ITU-R Recommendation P.676-12 (2019). Attenuation by atmospheric gases and related effects.

[i.2] ITU-R Recommendation P.840-7 (2017). Attenuation due to clouds and fog.

[i.3] ITU-R Recommendation P.838-3 (2005). Specific Attenuation Model for Rain for Use in Prediction Methods.

[i.4] ITU-R Recommendation P.530-18 (2021). Propagation data and prediction methods required for the design of terrestrial line-of-sight systems.

[i.5] Luini, L., Roveda, G., Zaffaroni, M., Costa, M., Riva C. (2018). EM wave propagation experiment at E band and D band for 5G wireless systems: preliminary results . Proceeding of EuCAP 2018, 9-13 April 2018, pp. 1-5, London, UK.

[i.6] Luini, L., Roveda, G., Zaffaroni, M., Costa, M., Riva, C. (2020). The Impact of Rain on Short E-band Radio Links for 5G Mobile Systems: Experimental Results and Prediction Models. IEEE Transactions on Antennas and Propagation, vol. 68, no. 4, Page(s): 3124-3134, April 2020.

[i.7] Lin, S. H. (1977). National Long Term Rain Statistics and Empirical Calculation of 11 GHz Microwave Rain Attenuation. Bell Syst. Tech. J., 56, 1581–1604.

[i.8] H. J. Liebe, G. A. Hufford, M. G. Cotton, 1993, “Propagation modelling of moist air and suspended water/ice particles at frequencies below 1000 GHz”, in Proc. AGARD 52nd Spec. Meeting EM Wave Propag

[i.9] D. Ahrens, 1994, “Meteorology Today: an introduction to weather, climate and the environment”, 9th edn. Brooks/Cole, Belmont.

[i.10] E. J. McCartney, “Optics of the Atmosphere: Scattering by Molecules and Particles”, New York: Wiley, 1976.

[i.11] L. Luini, C. Capsoni: “A Unified Model for the Prediction of Spatial and Temporal Rainfall Rate Statistics”, IEEE Transactions on Antennas and Propagation, vol. 61, no. 10, Page(s): 5249 - 5254, October 2013.

[i.12] T. Oguchi, 1983, “Electromagnetic wave propagation and scattering in rain and other hydrometeors”, Proc. IEEE, vol. 71, pp. 1029-1077.

[i.13] H.Y. Lam, L. Luini, J. Din, C. Capsoni, A. D. Panagopoulos, 2012, "Investigation of Rain Attenuation in Equatorial Kuala Lumpur", IEEE Antennas and Wireless Propagation Letters, vol. 11, Page(s): 1002-1005.

[i.14] M. M. Z. Kharadly, Robert Ross, "Effect of Wet Antenna Attenuation on Propagation Data Statistics", IEEE Transactions on Antennas and Propagation, Vol. 49, No. 8, Page(s): 1183-1191, August 2001.

[i.15] M. Thurai, V. N. Bringi, A. B. Manić, N. J. Šekeljić, B. M. Notaroš, 2014, "Investigating raindrop shapes, oscillation modes, and implications for radio wave propagation", Radio Sci., 49, 921-932

[i.16] R. Gunn and G. D. Kinzer, "The terminal velocity of fall for water droplets in stagnant air", J. Atmos. Sci., vol. 6, no. 4, pp. 243–248, 1949

[i.17] M. Rashid, Jafri Din, "Effects of reduction factor on rain attenuation predictions over millimeter-wave links for 5G applications", Bulletin of Electrical Engineering and Informatics, Vol. 9, No. 5, October 2020, pp. 1907~1915

[i.18] L. Luini and C. Capsoni, "The SC EXCELL model for prediction of rain attenuation on terrestrial radio links," Electron. Lett., vol. 49, no. 4, pp. 307–308, Feb. 2013.

[i.19] A. Musthafa, L. Luini, C. Riva, S, Livieratos, G. Roveda, "A Long-Term Experimental Investigation on the Impact of Rainfall on Short 6G D-Band Links", Radio Science, May 2023

3 Abbreviations

For the purposes of the present document, the following abbreviations apply:

3GPP	3rd Generation Partnership Project
5G	5th Generation of Mobile Networks
CCDF	Complementary Cumulative Distribution Function
DSD	Drop Size Distribution
EHF	30-300 GHz range (mm-wave range)
mmW	Millimetre Wave
MW	Microwave
PtP	Point to Point
SC EXCELL	Stratiform/Convective EXponential CELL
SHF	3-30 GHz range (cm-wave range)

4 Propagation features at mmW

4.1 Tropospheric attenuation

The atmosphere is a thermodynamic system containing water in vapor, liquid and solid state, gases and aerosol, surrounding the Earth up to 100 km. As for the propagation of millimeter-waves and microwaves along terrestrial paths, only the lower layer close to the Earth surface is of concern. The atmosphere is commonly characterized through temperature, pressure, relative humidity and density of its main components (gases and water).

4.1.1 Gaseous attenuation

Oxygen and water vapour are the gaseous components of the atmosphere influencing the electromagnetic wave propagation in the frequency range from 10 up to 350 GHz. Other gases need to be taken into account only at higher frequencies (e.g. CO2 for optical wavelengths). The weather condition with no fog is typically referred to as “clear sky” condition.

The oxygen absorption is mainly due to the resonance of oxygen molecules as magnetic dipoles, which occurs in specific bands: for example, oxygen attenuation is basically negligible up to 40 GHz, but it becomes important around 50 GHz and is dominant around 60 GHz.

The oxygen concentration depends on the air pressure and temperature. The former is characterized by a decreasing exponential profile with the height, while the latter is highly influenced by daily, seasonal and geographical variations. Oxygen absorption increases with the decrease in temperature.

The water vapour absorption, due to the molecular interaction with electromagnetic waves as electric dipole, can be calculated as the sum of two terms, which are linear and quadratic functions of the water vapour density, respectively. Water vapour absorption is linked to meteorological parameters like pressure, temperature and water vapour density.

In principle, the procedure to calculate the gaseous attenuation along terrestrial paths consists in two steps:

1) calculation of the specific attenuation due to gases γ_G (dB/km) at any point along the propagation path;

2) calculation of the total path attenuation due to gases A_G by integration of all the contributions.

In practice, this approach is unfeasible because it would require the knowledge at any time of the complete spatial distribution along the path of meteorological parameters like air pressure, temperature and gases concentration. However, as the attenuation due to gases is very stable in space (tens of kilometers) and in time (hours), γ_G is typically considered to be constant along terrestrial propagation paths, which is more and more true for short links (e.g. less than 1 km). In turn, this implies that the path attenuation can be simply calculated as:

$$A_G = \gamma_G L$$

where L (km) is the length of the terrestrial link.

The most acknowledged methodology for the prediction of γ_G L is named MPM93 and was proposed by Liebe et al. in [i.8]. The model, which is currently adopted in Annex 1 of recommendation ITU-R P.676-12 [i.1], defines the intensity and the width of oxygen and water vapor spectral absorption lines in the 1-1000 GHz frequency range. The contribution of each line, which depends on pressure P, relative humidity RH and temperature T, is summed up to yield the overall specific attenuation due to gases.

The specific attenuation due to gases, calculated using the Liebe MPM93 model is shown in Figure 1, for the following standard reference meteorological parameters: T = 15 °C, P = 1013.25 mbar and water vapor content (which is tighly linked to RH) ρ_V = 7.5 g/m3.

As is clear from the figure, the contribution coming from oxygen is mainly limited to the frequency bands around 60 GHz and 120 GHz, where the specific attenuation can reach values as high as 15 dB/km. On the other hand, the impact of water vapor is associated to three main absorption peaks (centered approximately around 22, 183 and 325 GHz), but it is also given by a linear term providing, in general, more attenuation than the one induced by oxygen (see especially the 210-310 frequency range).

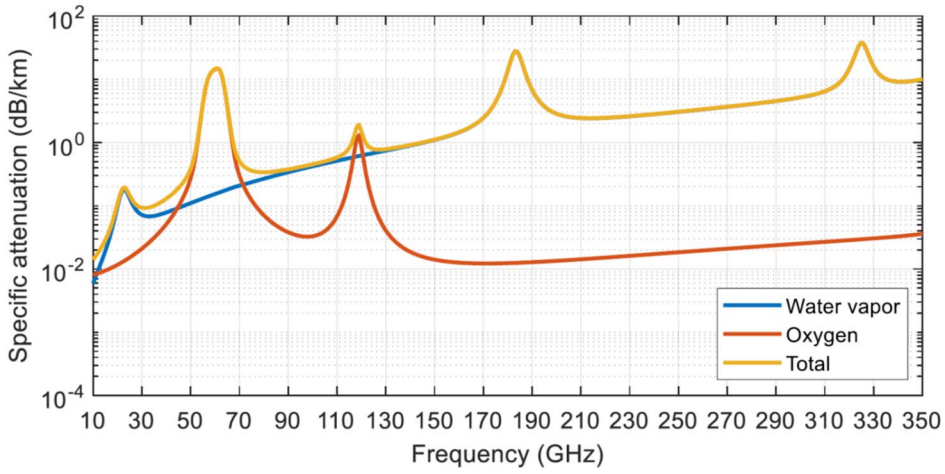

Figure 1: Specific attenuation due to gases as a function of frequency, calculated using the Liebe MPM93 model [i.8]

4.1.2 Fog attenuation

Fog is a suspension of microscopic water droplets (in the order of microns) formed by condensation of the atmospheric water vapor on the surface of suspended hygroscopic particles, named condensation nuclei. Fog is usually associated with values of relative humidity close to saturation (100%).

In meteorology, the term fog is used when the visibility is less than 1 km, whereas mist is an intermediate state where the relative humidity is above 60% and the visibility exceeds 1 km. Finally, haze is any suspension of dry solid particles (smoke, dust, sand, salt, etc.) of microscopic size. Fog, produced by cooling of the air, can be classified into [i.9]:

• Radiation fog: generated by radiational cooling of the Earth surface that lowers the air temperature enough to reach saturation. It is usually observed at night during the cold season and in calm wind conditions and it is typical of continental areas.

• Advection fog: due to a wet and warm air mass moving over a cool surface. It is more frequent during spring and requires moderate or fresh breeze blowing. It is further divided into marine fog (produced by advection of marine air from warm to cold oceanic areas) and coastal or maritime fog (originated by warm air masses migrating inland from the sea).

• Upslope or hill fog: due to adiabatic cooling of air masses moved up by wind along hill or mountain flanks.

The effects of suspended water droplets on EM waves is markedly different from the one induced by gases. Every droplet has a twofold impact on the incoming EM wave: part of the electromagnetic energy is scattered in several directions around the particle, while part of it is absorbed by the particle itself, causing an increase in its temperature. In general in the microwave and mmW region absorption prevails over scattering and the Rayleigh model applies [i.10].

The dimension of the water droplets forming fog is very small: they are in the order of microns. When considering EM waves in the 10-300 GHz, the shortest wavelength is λ = 1 mm (for f = 300 GHz), which is three order of magnitude larger than the size of fog droplets.

The specific attenuation due to fog γ_F is shown in Figure 2 as a function of frequency, for different liquid water contents (where T is fixed to 0 °C) [i.2].

The impact of fog increases continuously with frequency, reaching up to 7 dB/km at 300 GHz with w = 0.5 g/m3, which is considered as the limit value associated to extremely thick fog.

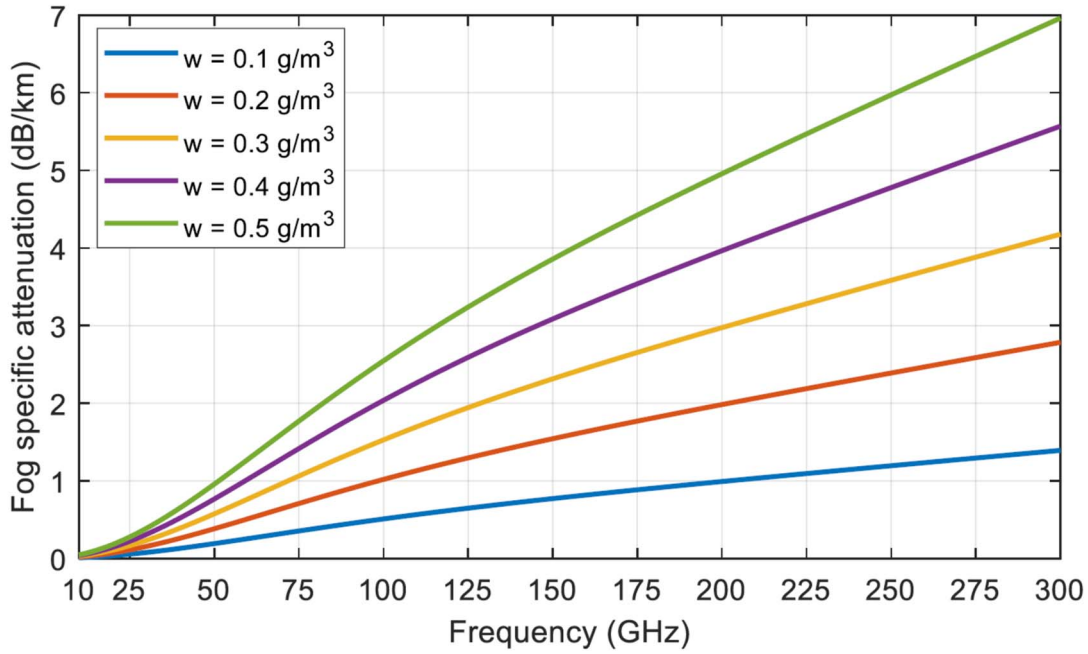

Figure 2: Specific attenuation due to fog (T = 0 °C) as a function of frequency and for different liquid water content values [i.2]

4.1.3 Rain attenuation

Rain is the prevailing phenomenon related to precipitating particles in the atmosphere and, depending on the site, it occurs for a period of time approximately comprised between 1% and 10% in a year (the year is considered as the basic repetition period for weather phenomena). Values as large as 3%-7% are quite common in temperate climates [i.11]. Rain affects the lower part of the atmosphere; specifically, making reference to temperate climates, rain develops up to a few kilometers during winter because of the low height of the 0 °C isotherm layer (usually assumed as the vertical limit for the presence of water particles during stratiform events) and up to 10-15 km during thunderstorms (typical of summer periods) because of the strong updrafts/downdrafts which carry water/ice particles even to the highest layers of the atmosphere.

Rain consists of drops of spheroidal shape with equivolumetric diameters varying between few tenths of millimeters to a maximum of 6 millimeters (larger drops are not common because the cohesive force is not as strong as the aerodynamical force). In fact, the hydrometeor shape is far from being spherical if its dimension is large, because of the balance between the internal and external forces acting on the lower surface of the drop in its falling path. Measurements have shown that drops larger than about 1 mm in radius are of oblate spheroidal shape with flattened base [i.12].

As an example, Figure 3 depicts the typical shape of a falling rain drop, for different sizes. The black line represents the most probable shape derived from several drops within the same size class (figure extracted from [i.15]), which points out that the oblateness increases with the drop dimension.

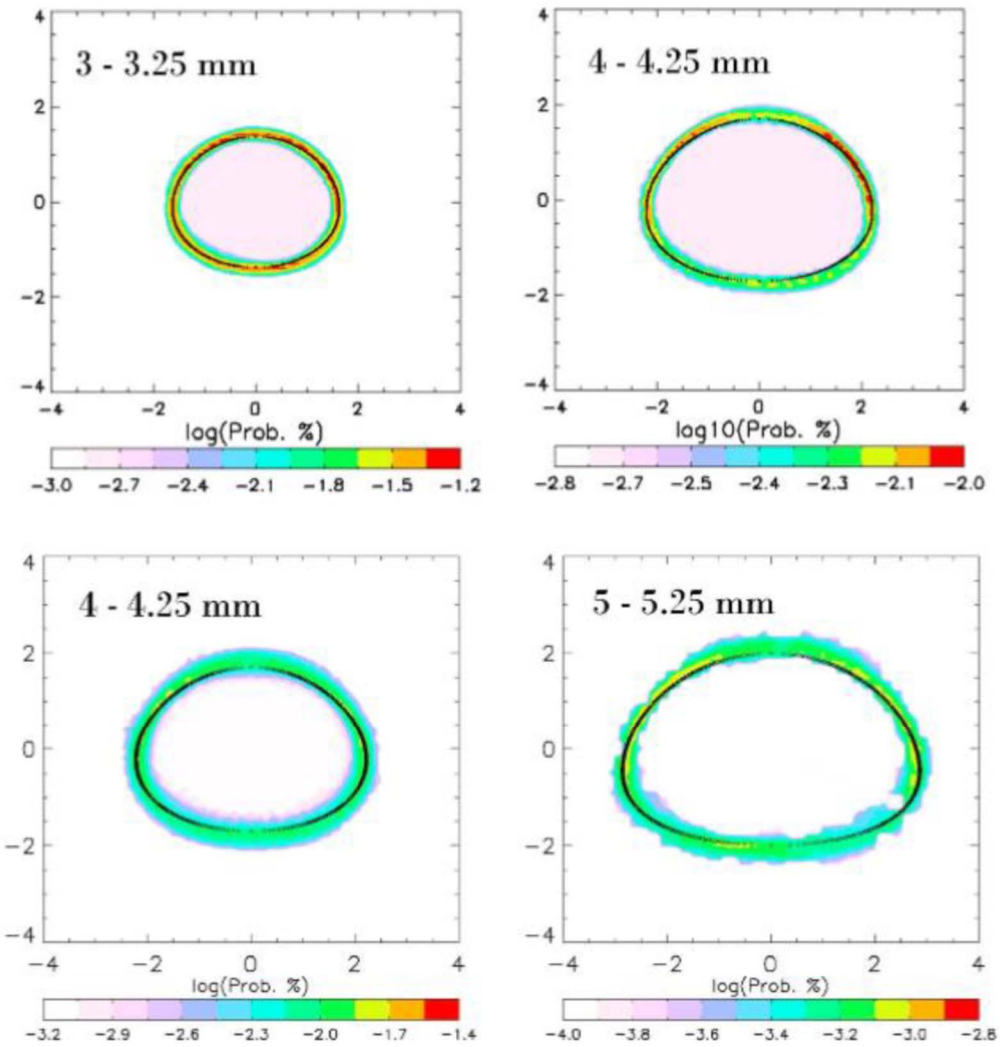

Figure 3: Typical shape of falling rain drops, for different sizes; the black line represents the most probable shape derived from several drops within the same size class [i.15]

For what concerns the impact of hydrometeors on electromagnetic waves, rain represents the main drawback to their propagation at frequencies above 10 GHz because the hydrometeor size is comparable with the wavelength of the incident wave. Other types of precipitation such as hail and snow are not considered in this report because their effects on the propagation of the electromagnetic waves are marginal and their occurrence probability well below the one of rain.

Each rain drop causes scattering and absorption (i.e. attenuation, overall) on EM waves, however, contrary to the water droplets forming fog, the size of rain drops is of the same order of the wavelength considered in the 10-350 GHz range (millimeters for both). This has a twofold effect: on one side, absorption and scattering are comparable and, on the other side, the specific attenuation due to rain, γ_R, has a more complex expression compared to the case of fog. Indeed, γ_R depends on the size of each drop as follows [i.13]:

$$\gamma_R = 4.343 * 10^3 \int_D \sigma_{ext}(D, f) N(D) dD$$

where σ_{ext} is the extinction cross section, taking care of both scattering and absorption, D is the rain drop diameter, N is the number of drops with diameter D, f is frequency.

This equation points out that the specific attenuation due to rain is obtained by weighting the fade induced by a rain drop with given diameter D with the number of rain drops with that size. This latter information is provided by N(D) (typically referred to as Drop Size Distribution − DSD), which indicates the number of rain drops with given diameter D contained in 1 m^3. The DSD, whose units are mm^{-1} m^{-3}, is typically measured by specific instruments, named

disdrometers, which count and classify drops according to their size; the DSD can be derived from the output of a disdrometer as follows [i.13]:

$$N(D_i) = \frac{10^6 n_i}{Sv(D_i)T\Delta D_i}$$

In (2-23), n_i is the number of raindrops whose diameter falls in the i-th class (with mean diameter D_i), ΔD_i (mm) represents the width of each drop-size class, S (mm^2) is the disdrometer sampling area, T (seconds) is the instrument integration time, $v(D_i)$ (m/s) is the terminal velocity of rain drops, which, for example, can be extracted from the work of Gunn and Kinzer [i.16] or derived directly from the disdrometer measurements.

Besides measured from a disdrometer, the DSD can also be modelled using analytical functions. According to the ratio of the size of the drop to the wavelength inside the particle and to the shape of the drop, different electromagnetic techniques can be used to compute the extinction cross section σ_{ext}. In fact if drops are small with respect to the wavelength, the Rayleigh scattering approach can be used; if they are large, but spherical, the exact Mie solution can be applied; in the most general case, including oblate spheroids, approximate numerical methods have to be used.

As extensively shown in the literature [i.3], [i.13], the specific attenuation due to rain γ_R, obtained for different rain intensity values R (mm/h), can be fitted with good accuracy using the following power law equation:

$$\gamma_R = kR^{\alpha}$$

where k and α are coefficients that depend on the operational frequency f, the wave polarization (linear vertical for terrestrial links) and link elevation (zero for terrestrial links).

It is worth mentioning that this approach assumes that the rain rate, measured at the receiver side, is constant along the whole path: this hypothesis is definitely acceptable for stratiform events (roughly, when the peak rain rate does not exceed 10 mm/h), while it might be more questionable for convective events; in this case, the introduction of a path reduction factor represents a simple yet effective way of taking into account the spatial inhomogeneity of the rain rate along the path (more details are discussed in Section 6.2).

The specific attenuation due to rain γ_R is shown in Figure 4 as a function of frequency, for different rain rates, calculated according to recommendation ITU-R P.838-3 [i.3]: while specific attenuation increases monotonically with R, reaching even values as high 50 dB/km for 200 mm/h (f ≈ 115 GHz), γ_R increases with frequency up to 100 GHz, after which, depending on R, a stable or slightly decreasing trend emerges.

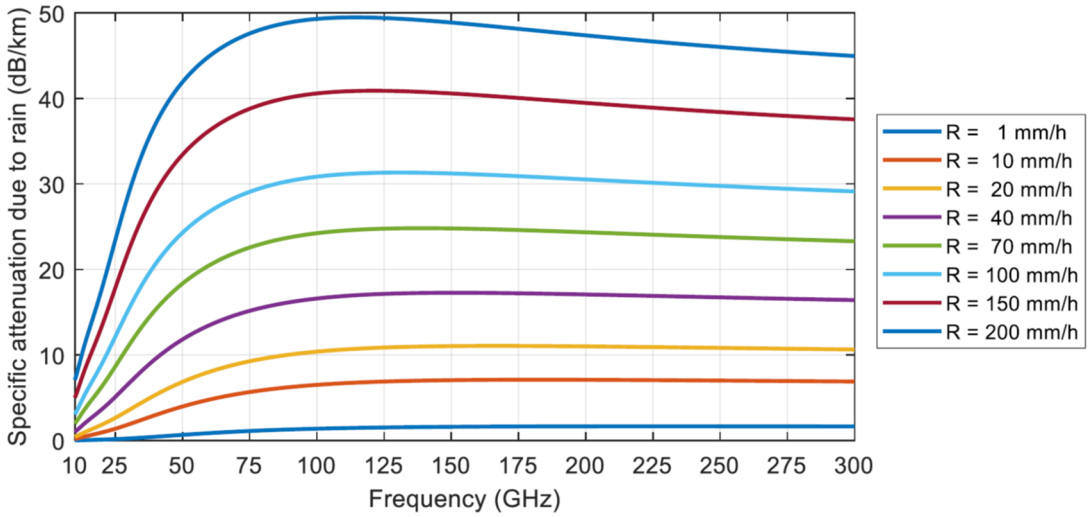

Figure 4: Specific attenuation due to rain as a function of frequency, for different rain rates, calculated according to recommendation ITU-R P.838-3 [i.3]

It is important to note that the attenuation curves shown in Figure 4 are actually just a reference to give a hint about how intense the fades caused by rain can be. Indeed, an accurate evaluation of the specific attenuation γ_R is to be done not simply as a function of rain rate R but more precisely as a function of DSD.

From the physical point of view as long as the wavelength is much larger than the rain drop size, as it is in the cm-wave range, the Rayleigh scattering prevails and the rain attenuation is related to the total volume of water in the raindrops,

that is to the rain rate, with the distribution of drop size being hardly relevant; instead when the wavelength becomes comparable with the drop size, as it is in the mm-wave range, Mie scattering becomes more relevant and the rain attenuation gets more sensible to the actual distribution of drop size.

A comparison among different models is shown in next section on the base of experimental data.

5 Rain attenuation prediction: event-based analysis

This section presents different methods that can be used to predict the time series of the rain attenuation starting from information on precipitation.

As we noted in section 4.1.3 there are two models that can be applied to predict the rain attenuation:

- A model based on a power law equation which is employed in recommendation ITU-R P.838-3, where the specific attenuation due to rain γ_R is only function of rain rate R and frequency
- A model considering the specific attenuation due to rain γ_R as a function of Drop Size Distribution

In order to compare the accuracy of the two models a propagation experiment has been carried out since 2016 and is still ongoing at Politecnico of Milan [i.5] considering a link with radios at E band (about 80 GHz) and D band (about 150 GHz) co-sited. The link length is about 325 m and measurement instruments are present on site such as a disdrometer, which allows to measure DSD, and a radiometer, which allows to measure pressure P, temperature T and relative humidity RH.

The attenuation due to rain can be derived by measuring the received power at one link side and by evaluating the attenuation due to gases by means of Liebe MPM93 model (see section 4.1.1) and from the measurement of P, T and RH. The attenuation due to rain as measured by the radio link can be compared to the one predicted by ITU-R P.838-3 and to the one predicted by disdrometric data for different rain events.

5.1 Wet antenna effect

In order to perform the comparison between models with the measured rain attenuation, the so-called wet antenna effect has to be properly evaluated and filtered out of the measurement. When it is raining, a thin layer of water can be deposited over the surface of the antenna radome of the radio link, provoking an attenuation that is not related to propagation.

This effect has been modelled in [i.14], where the attenuation grows with rain rate till a stationary value according to a simple exponential law:

$$A_{wa} = a(1 - e^{bA_T})$$

where A_T is the total attenuation obtained from the received power, a and b are coefficients depending on frequency and type of antenna radome and coating.

In the propagation experiment at Politecnico of Milan [i.6], the wet antenna effect has been evaluated and filtered out from measured rain attenuation by leveraging on data collected by the disdrometer during stratiform rain events, during which the rain rate can be assumed as constant over the link length. In Figure 5 the evaluated wet antenna attenuation on one link at E band is reported.

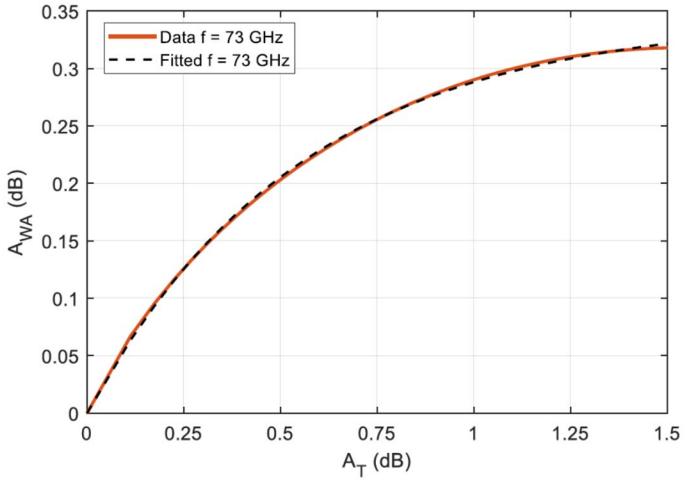

Figure 5: estimated wet antenna attenuation as a function of total link attenuation got from disdrometer data (red line) and fitted by the power law coefficients at 73 GHz [i.6]

The wet antenna effect can be significantly reduced by using a suitable coverage and/or hydrophobic coating of the radome.

5.2 Comparison of models

A first sample of comparison among rain attenuation models at E band is given by the propagation experiment at Politecnico of Milan [i.5] and shown in Figure 6 considering:

- the data measured by the radio link as a reference
- the data predicted by ITU-R P.838-3
- the data predicted by the model based on DSD got by the disdrometer

with respect to the measured rain rate reported in figure 7.

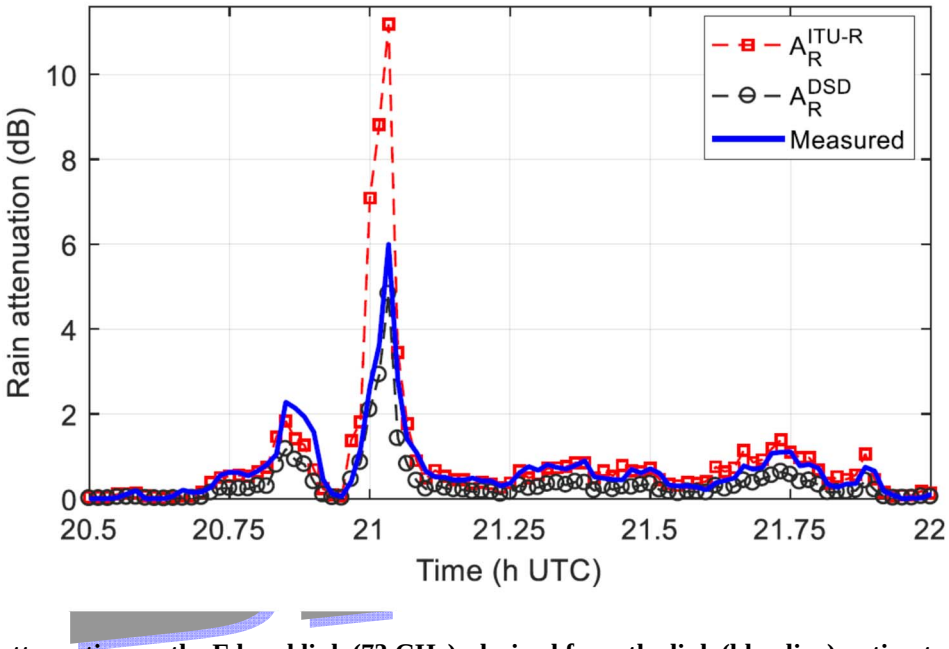

Figure 6: Rain attenuation on the E band link (73 GHz): derived from the link (blue line), estimated by rain rate using ITU-R P.838-3 (red line) and estimated by DSD data (black line) [i.5]

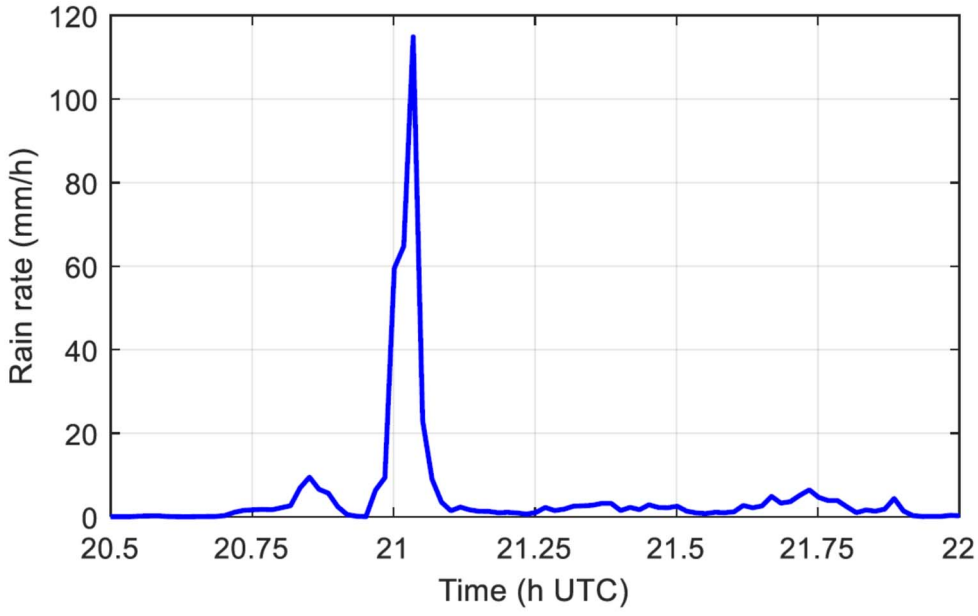

Figure 7: Measured rain rate [i.5]

As it can be seen the model based on DSD data gives a much better estimation of the rain attenuation than the model from ITU-R P.838-3; this is due to the strong impact of DSD: with a very intense rain event (about 115 mm/h) the ITU-R P.838-3 model tends to overestimate the rain attenuation.

A second sample of comparison at D band is shown in Figure 8 with reference to the rain rate reported in Figure 9.

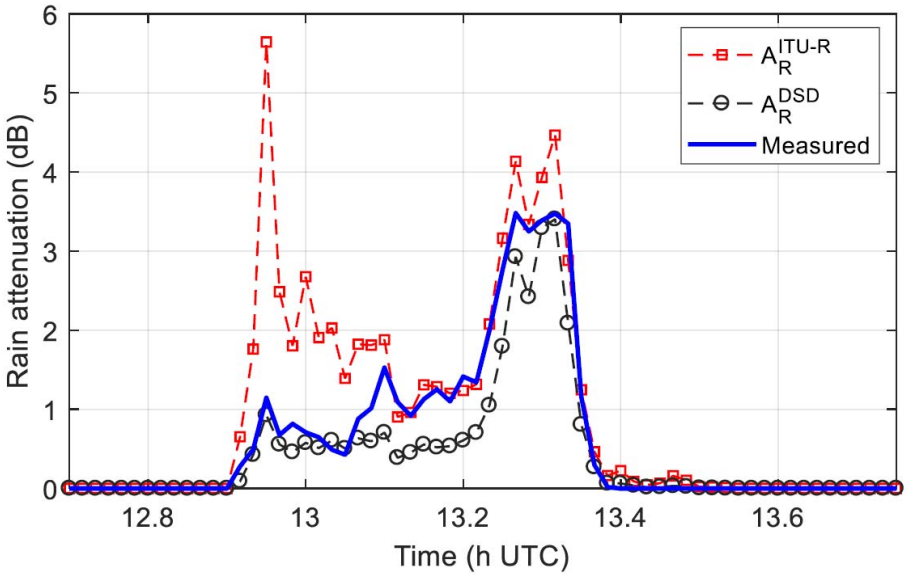

Figure 8: Rain attenuation on the D band link (148 GHz): derived from the link (blue line), estimated by rain rate using ITU-R P.838-3 (red line) and estimated by DSD data (black line) [i.5]

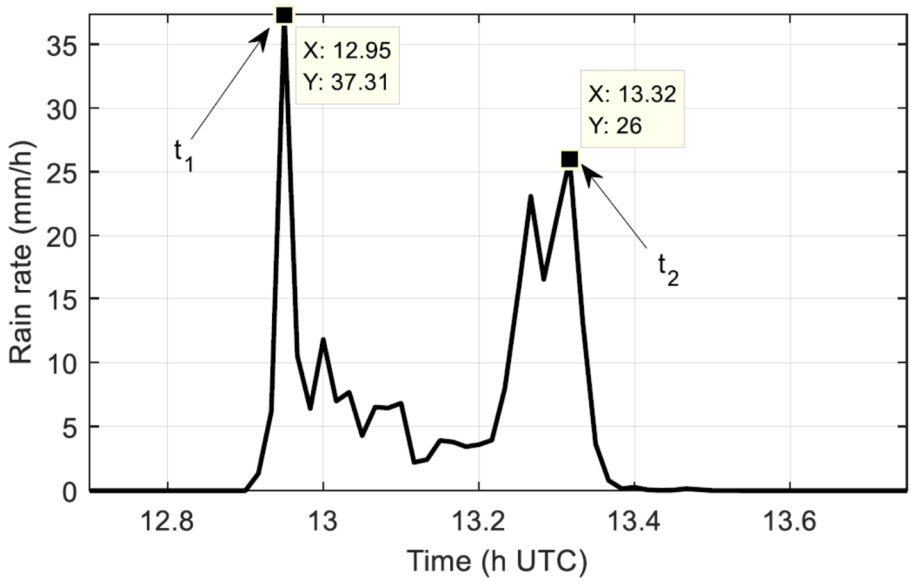

Figure 9: Measured rain rate measured [i.5]

Also in this case a significant overestimation of the rain attenuation is obtained by the ITU-R P.838-3 model, whilst the model based on DSD data is much more accurately following the measured curve.

It is interesting to investigate the different rain attenuation behaviours during the two different rain rate peaks; this comes out to be a consequence of the microphysics of the rain drops, as can be seen in Figure 10:

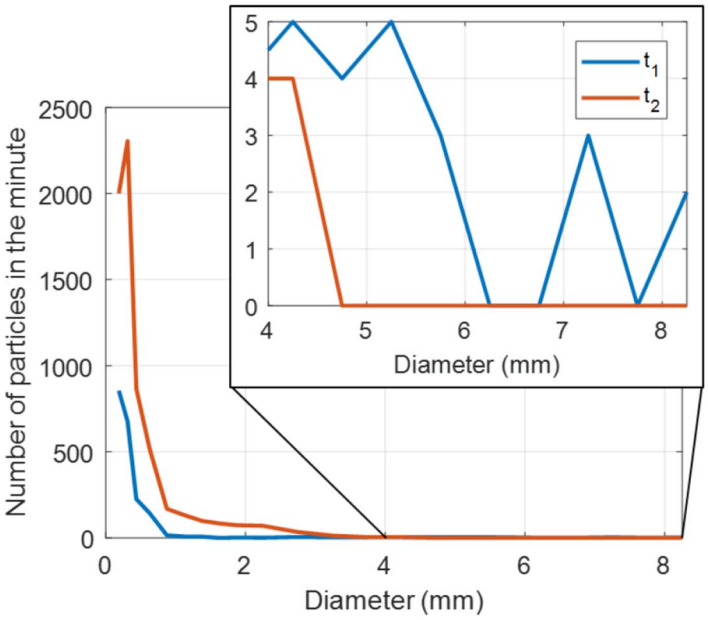

Figure 10: DSD relative to the two rain rate peaks labelled as t1 and t2 in Figure 9

While the DSD of t_2 contains much more small drops than that of t_1, the key difference between the two spectra lies in the large rain drops measured in t_1, but not in t_2, i.e. those for which D > 4 mm. Though not many, such large drops have a dramatic impact in increasing the value of rain rate, while definitely quite a limited one on the rain attenuation.

This sample case definitely highlights the importance of using DSD data to achieve high accuracy in predicting rain attenuation. In particular at mmW, small (e.g. D around 0.5 mm) and large (e.g. D around 3 mm) drops definitely have a different impact, which the information on the DSD allows to properly weight in calculating specific attenuation due to rain.

6 Rain attenuation prediction: statistical analysis

The methods presented in the previous section allow estimating the time series of the rain attenuation, but the main drawback of such approaches is obviously the need for the rain rate time series. Indeed, this kind of data is seldom available worldwide, even more with the necessary temporal resolution (at least 1 minute); on the other side, the statistical approach to link design can be achieved with simpler input data and it provides the atmospheric link margin to guarantee a given link availability.

This section is devoted to investigating the accuracy of some statistical prediction models, specifically:

- the model adopted by ITU-R Recommendation P.530-18 [i.4], typically used as a reference for terrestrial link design
- the Lin model [i.7], already showing a good prediction accuracy when used to estimate rain attenuation statistics at E band [i.6]
- the Abdulrahman model and the Da Silva Mello model [i.17]
- the SC EXCELL model [i.18], which represents analytically rain as a set of exponentially decaying shaped rain cells

It is worth remembering that, actually, the application of the ITU-R model is recommended for operational frequencies up to 100 GHz.

6.1 Impact of path reduction factor

Rain occurs in cells with the rain rate higher at the center of the cell and decreasing going to the edge of the cell, where the decrease rate is higher with convective events and lower with stratiform events.

As a consequence, in order to predict correctly the attenuation due to rain, the spatial distribution of the rain precipitation along the link length is to be considered. The attenuation due to rain can be expressed as:

$$A_R = \gamma_R L_{eff} = \gamma_R L r$$

where L_{eff} is the effective length over which the rain rate can be considered homogeneous, L is the link length and r is the path reduction factor.

Different expressions of path reduction factor are given by different models; in particular in ITU-R P.530-18 it is expressed as:

$$r = \frac{1}{(0.477\, d^{0.633}\, (R_{0.01\%})^{0.073\alpha}\, f^{0.123} - 10.579\, (1 - e^{-0.024 d})}$$

where d is the link length, f is the frequency, R is the rain rate exceeded for 0.01% of the time, α is the parameter within γ_R.

Instead in the Lin model it is expressed as:

$$r = \frac{1}{1 + d/(\frac{2632}{R_p - 6.2})}$$

where R_p is the rain rate exceeded for p% of the time.

The different behaviour of path reduction factor with link length and rain rate can be clearly understood looking at Figure 11 (model in ITU-R P.530-18) and Figure 12 (Lin model), where on the left the behaviour is described on a 5 km span whilst on the right there is the detail up to 350 m link length [i.18].

In both cases the expected decrease of path reduction factor with rain rate is observed, since the higher is the rain rate, the more convective is the event, the more uneven is the spatial distribution of the rain rate along the path.

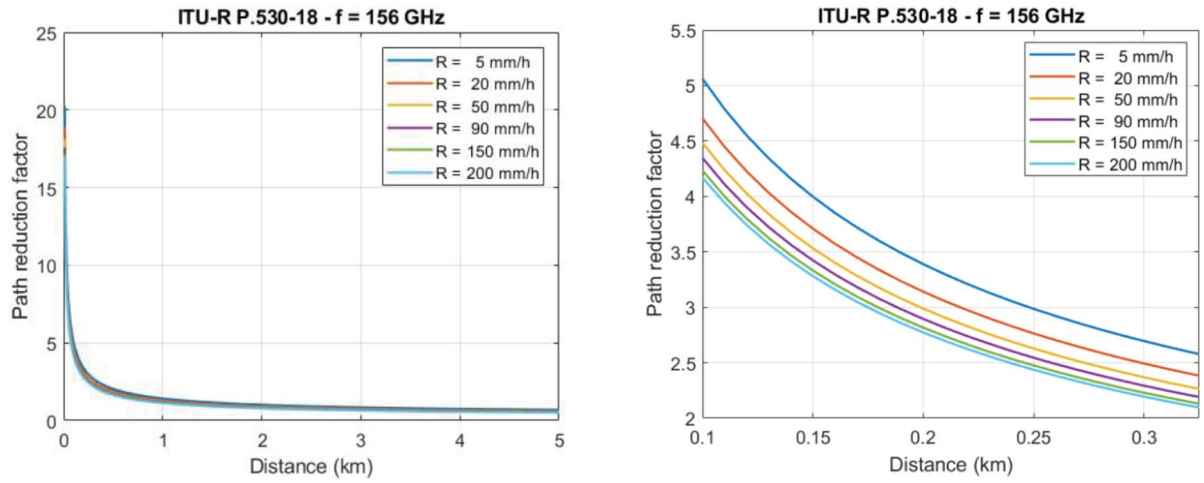

Figure 11: path reduction factor as a function of link length according to the model in ITU-R P.530-18 [i.19]

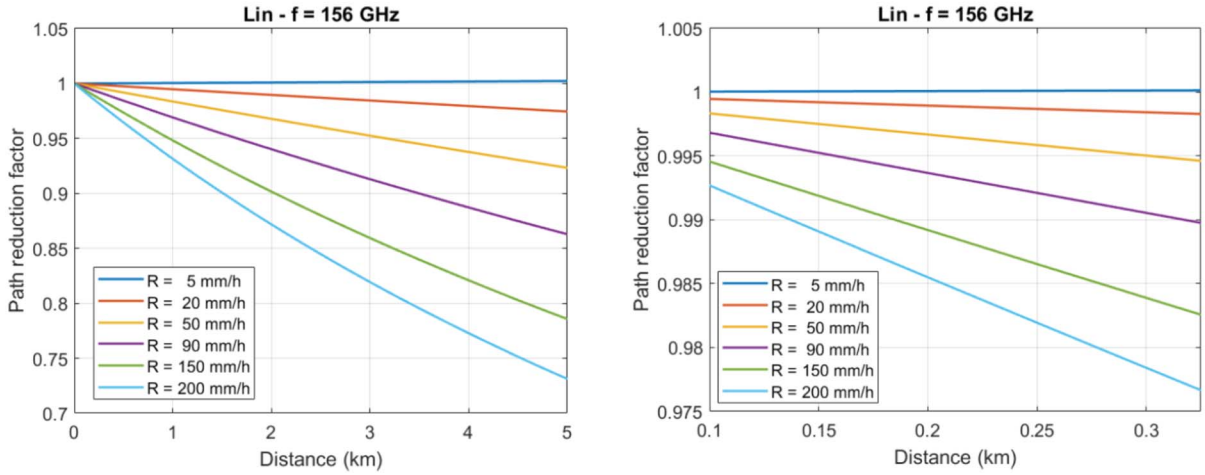

Figure 12: path reduction factor as a function of link length according to the Lin model [i.19]

The difference in the evaluation of the path reduction factor between the two models is particularly huge when considering short links (less than 1 km) where r grows exponentially well over 1 with decreasing link length in the ITU-R model, whilst it remains slightly less than 1 in the Lin model.

This discrepancy has been found also in other analysis considering alternative models, such as the Abdulrahman model and the Da Silva Mello model [i.17]. These models share with the Lin model a path reduction factor less than 1 for link length shorter than 1 km, as shown in Fig. 13.

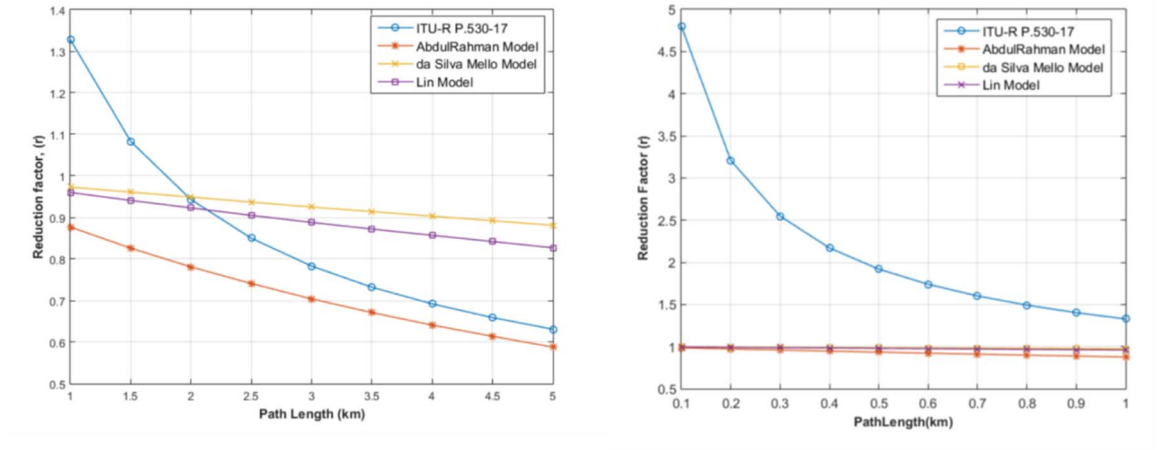

Figure 13: path reduction factor as a function of link length according to different prediction models [i.17]

6.2 The SC EXCELL model

ITU-R Recommendation P.530-18 as well as Lin, Abdulrahman and Da Silva Mello models are all derived by different regression techniques trying to fit real measured data.

Another approach to modelling is to start from a mathematical description of rain to get a proper statistical prediction. One example of this way of proceeding is the SC EXCELL model [i.18], which describes rain as a set of rain cells with an exponential decay of the rain rate and rotational symmetry, where the probability of occurrence of each rain cell is uniquely identified by its peak rain rate R_M (mm/h) and its effective dimension ρ_0 (km):

$$R(\rho) = R_M e^{-\frac{\rho}{\rho_0}}$$

The peak value and the steepness of decay of a rain cell are dependent on the type of rainfall: on one side convective rain is expected to have high peak and fast decay, on the other side stratiform rain would show low peak and slow decay.

The description of the rain environment is completed by introducing the probability of occurrence N of the rain cells, which is a function of the two parameters univocally defining each cell (R_M and ρ_0) as well as of the local rainfall complementary cumulative distribution function of rain rate.

Thanks to its physical soundness in representing the rainfall environment, the SC EXCELL method does not require any calibration procedure on existing data, as is typically the case of most of the semi-empirical models considered.

The performance of the SC EXCELL prediction model has been evaluated [i.18] against the global DBSG3 database of ITU-R, which includes concurrent rain rate and rain attenuation statistics collected in several sites worldwide, showing an improvement in the prediction accuracy with respect to the method currently recommended by ITU-R (P.530-18).

6.3 Comparison of models

In order to compare the different available models for the prediction of rain attenuation, a statistical analysis based on the collection of long term rain data is valuable.

In the framework of the propagation experiment at Politecnico of Milan [i.6] full year data have been collected for the links at E and D band.

The complementary cumulative distribution function (CCDF) of the rain attenuation measured and estimated at 73 GHz and 83 GHz over 1 year observation period (from February 2017 to January 2018) are shown respectively in Fig. 14 and 15, whilst the CCDF of the rain rate measured by the disdrometer over the same period is shown in Fig. 16.

In particular the curves compared in the figures describe:

- the model provided by Recommendation ITU-R P.530 considered with rain rate exceeded for 0.001% of the time both measured locally ($R_{0.001\%}$ = 41.9 mm/h) and derived by Recommendations ITU-R P.837-7 and ITU-R P.838-3
- the SC EXCELL model
- the Lin model
- the data measured by the disdrometer

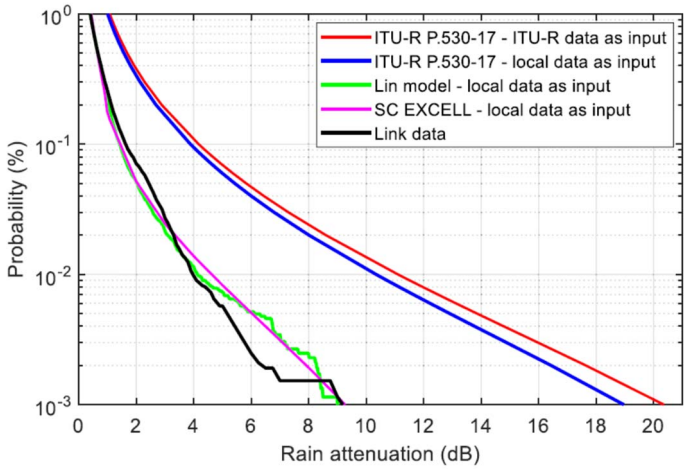

Figure 14: comparison between the rain attenuation CCDF measured using the link and estimated by prediction models; f = 73 GHz [i.6]

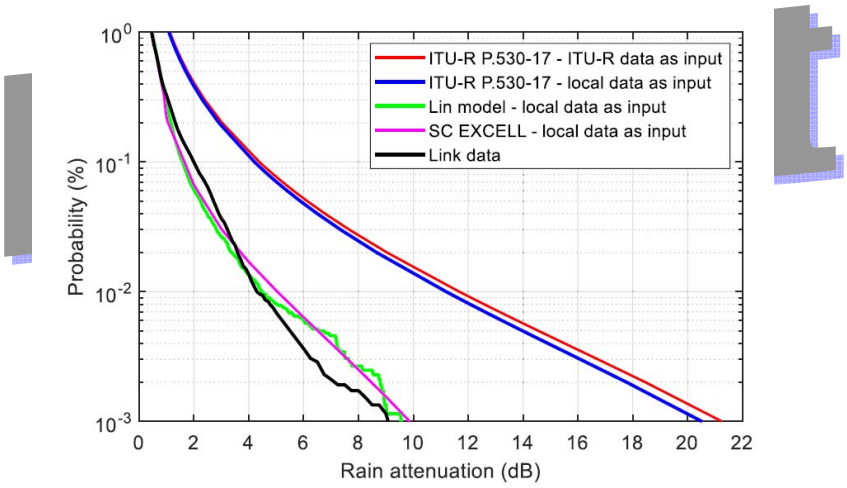

Figure 15: comparison between the rain attenuation CCDF measured using the link and estimated by prediction models; f = 83 GHz [i.6]

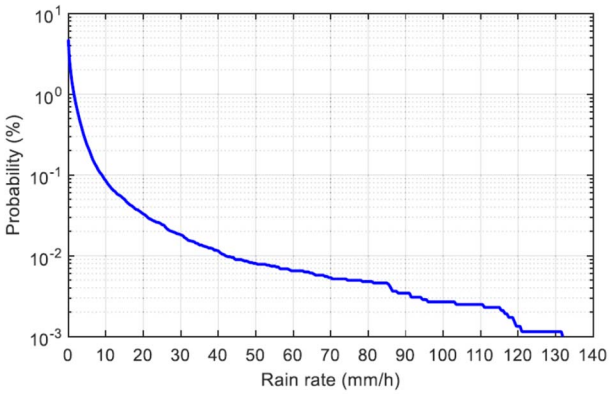

Figure 16: CCDF of the rain rate as measured by the disdrometer in Milan in the period February 2017–January 2018 [i.6]

As is clear from Fig. 14 and 15, in comparison with the measured data both the SC EXCELL and Lin models provide accurate predictions, whilst the ITU-R 530 model largely overestimates the measured data. This is likely due to the very high values of the path reduction factor r, which, for the above tests, ranges between 2.34 (f = 83 GHz) and 2.5 (f = 73 GHz).

It is worth noticing that the increased accuracy of both SC EXCELL and the Lin model is also partially due to the fact that they receive as input the full rain rate CCDF, while, on the contrary, the ITU-R model makes use only of $R_{0.01\%}$.

A similar behaviour has been found when considering two links both operating at 156 GHz [i.19]:

- one in Milan within the same propagation experiment considered above, with data collected between 01/02/2018 and 31/01/2020
- one in Athens, over a 100 m distance, with data collected between 01/10/2019 and 31/05/2021.

In this case a modified version of the ITU-R P.530 model has been considered as well, where the path reduction factor is limited to 1; with this modification the model fits very well to the measured data, as can be seen in figures 17 and 18.

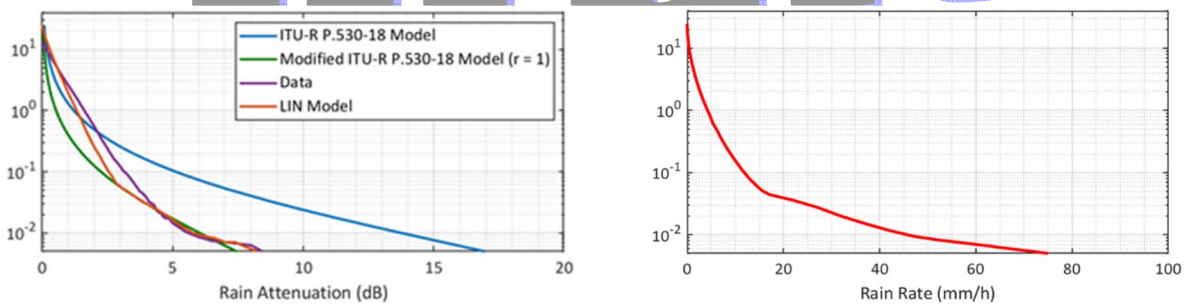

Figure 17: comparison between the rain attenuation CCDF measured using the link and estimated by prediction models, f = 156 GHz; CCDF of rain rate (link in Milan, 325 m) [i.19]

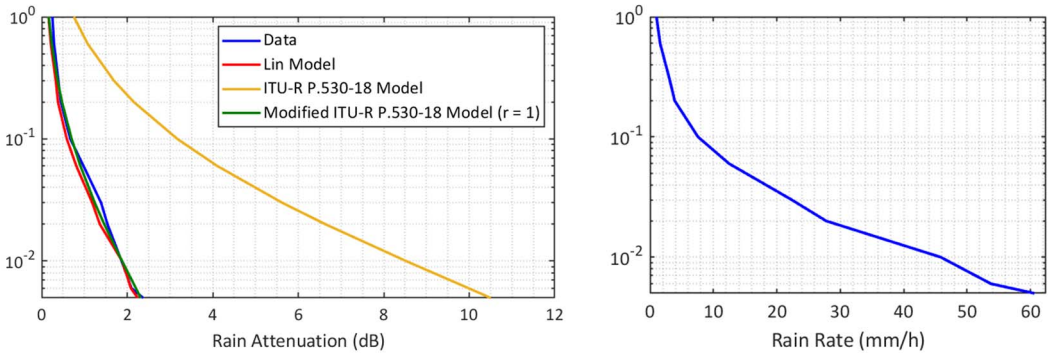

Figure 18: comparison between the rain attenuation CCDF measured using the link and estimated by prediction models, f = 156 GHz; CCDF of rain rate (link in Athens, 100 m) [i.19]

Considering that Athens and Milan are subject to different meteorological conditions and that the two links have different path lengths, the results shown in this analysis give a significant indication on the need to adopt a physically sound value for the path reduction factor in very short links, considering a value close to 1 when the rain rate can definitely be considered constant along the path.

7 Implications to radio link budget evaluation

A good model of the attenuation due to rain is very important in order to define the fade margin of a radio link with sufficient accuracy. When considering link budget at mmW, technological limitations on both transmitter maximum power and receiver sensitivity make the optimization of rain fade margin even more important.

From what seen in section 6 the currently adopted model within ITU-R Recommendation P.530-18 tends to overestimate the rain attenuation in particular when considering link lengths shorter than 1 km, due to a not physically sound consideration of the path reduction factor. In fact when rain rate can be considered constant along the path, the path reduction factor should be reasonably slightly less or equal to 1. This physical consideration is corroborated by long term measurements performed at both E and D band in Milan and Athens, but also by several other similar studies done in other parts of the world.

A proper adaptation of the P.530-18 model limiting the path reduction factor to 1 seems to be a good way forward to have an accurate prediction model usable for radio link budget evaluation.

8 Conclusions

Annex A (informative): Authors & contributors

The following people have contributed to the present document:

Rapporteur (and Editor):
Mr. Giuseppe Roveda, Huawei Technologies Italy

Other contributors:
Prof. Lorenzo Luini (Politecnico of Milan)

Prof. Carlo Riva (Politecnico of Milan)

History

Document history		
<Version>	<Date>	<Milestone>
0.0.1	25-05-2023	First draft in ETSI format
0.0.2		
0.0.3